

DD

INFN – Istituto Nazionale di Fisica Nucleare
Sezione di Genova

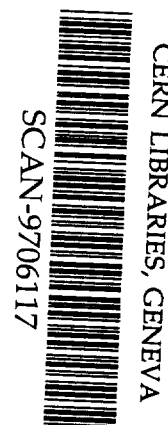
INFN/BE-97/03
10 Aprile 1997

**THE PROTON AND DEUTERON POLARIZED TARGET FOR CLAS:
PRELIMINARY RESULTS AT THE UNIVERSITY OF GENOA**

M. Anghinolfi*, P. Cocconi*, D.G. Crabb*, R. De Vita*, F. Parodi*, A. Rottura*

*I.N.F.N.– sezione di Genova, Via Dodecaneso 33, I-16146 – Genova

* Physics Department, University of Virginia, Charlottesville, VA 22901, USA



swy725

Abstract

Inclusive and seminclusive electron scattering experiments with polarized beam and targets are planned to run in hall B at TJNAF starting from 1998.

Within this program, the INFN group of Genoa will provide part of the solid state target where both proton and deuteron nuclei will be polarized.

In this report we present the preliminary result on the proton polarization of a butanol sample obtained with the Dynamic Nuclear Polarization method in our laboratory in Genoa.

1 – INTRODUCTION

The University and the National Institute for Nuclear Physics of Genoa participate to the Italian experimental activity at TJNAF (AIACE collaboration) providing, together with the Frascati group, the two modules of the large angle calorimeter (LAEC)[1] of CLAS[2], the 4π detector in Hall B: these modules are now installed and the conditioning period is started.

At present, in collaboration with the University of Virginia and TJNAF, we are considering the realization of a polarized target to be installed in CLAS. This device will ‘unfroze’ the

experiments which require a polarized beam and target[3]: these measurements, of prominent physical interest, have been highly rated by different PAC and we will participate to them in a leader position.

Polarized target to be used in extracted beam are nowadays available in different international laboratories including CERN[4] and SLAC: though realization, maintenance and reliability are well established[5], these systems are quite complex and involve different aspects like cryogenics, pumping, super conducting magnets, microwaves etc.

Therefore, in order to become familiar to this technology, we decided to install in our laboratory a minimal facility sufficient to polarize a sizeable sample of hydrogenous material.

In this report we present the set up of the experimental apparatus and the preliminary results we have obtained on a butanol target.

2 – THE EXPERIMENTAL APPARATUS

Since the target is designed to operate in combination to a low-intensity electron beam, the dynamic nuclear polarization (DNP) method [5,6,7] was followed.

In this approach an hydrogenous material containing a low concentration ($\approx 10^{19} / cm^3$) of 'free' paramagnetic electrons is maintained in a strong and uniform magnetic field (2.5 ÷ 5 Tesla) at low temperature ($\approx 1^0 K$). Under these conditions the polarization at thermal equilibrium (TE) is given by:

$$P_{TE} = \frac{\mu H}{KT} \quad (1)$$

where μ is the proton magnetic moment, K is the Boltzmann constant, H the magnetic field and T is the lattice temperature. For H=5 T and T=1⁰ K, P_{TE} =0.5 % for protons and P_{TE} =99% for electrons. To allow DNP to take place the sample is irradiated with microwaves (140 GHz @ 5 T) while a system based on the NMR is used to determine both the thermal equilibrium and the enhanced proton polarization.

2.1 – The target assembly

As shown in Fig. 1, the target holder consists of a Kapton square cylinder ($\varnothing = 2$ cm.) contained in a copper box connected to the wave guide by a conical trumpet to uniformly irradiate the sample. On the bottom of the box a spare empty space is also allocated.

The straight central wave guide is a 170 cm. length, 5 mm \varnothing CuNi tube supported by the top flange of the variable temperature insert (VTI) and by two 85 cm fibreglass sticks. The NMR signal to measure the polarization is transmitted by a semirigid CuBe cable (JT 50085) terminating in one single loop inside the Kapton cylinder. The helium level inside the VTI is monitored by a probe (CRYOGENIC HLG 200/210), while a CERNOX resistor (LakeShore CERNOX CX 1050 SD) measures the temperature of the helium bath immediately outside the copper target holder.

The complete transmission line of the microwaves (MW) is represented in upper part of Fig. 1: the symbols correspond to the dimensions of the guides and to the different options from MILLITECH company.

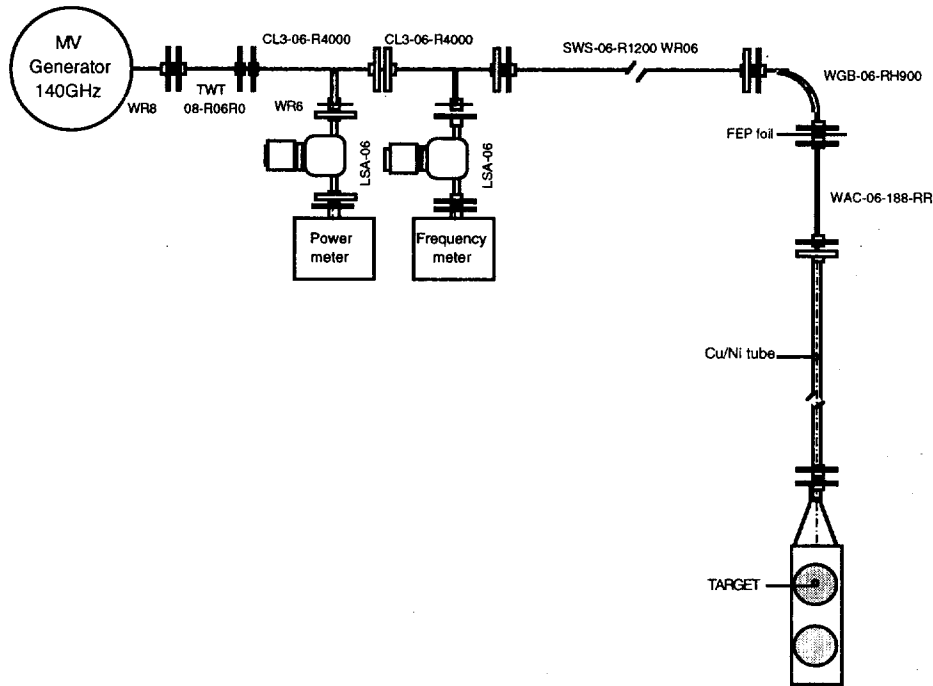


FIG. 1 – The MW system to irradiate the target. The characteristics of the wave guides, directional couplers and attenuators are indicated according to MILLITECH catalogue; the FEP foil separates the transmission line in open air from the portion in the VTI.

An EIO tube (CPI VKT 2438 PS) with the relative power supply (CPI VPW 2838) provides the MW source for the DNP giving an output power of 17 W in the 138–142 GHz frequency interval.

Two directional couplers are connected to a power meter (HP 432 A) and to a frequency counter (EIP 588 C). A FEP foil placed immediately above the top flange of the VTI separates the transmission line in open air from the portion in the VTI.

Different hydrogenous materials can be used to polarize protons. For our purpose we could obtain from the SMC collaboration at CERN a sufficient quantity of butanol beads doped with EHBA–Cr^v while polarization of deuterated materials is planned.

2.2 – The cryostat and the pumping system

The cryostat from CRYOGENIC Ltd. is equipped with a super conducting dipole magnet producing a maximum field of 6 Tesla with 0.1% uniformity in a few centimetre central region while the VTI is connected by a needle valve to the main helium tank allowing a flow rate greater

than 4 l/hr. On the top of the VTI, space is allocated for the flange supporting the target stick and for two 10 cm. \varnothing flexible tubes connecting the pumping system.

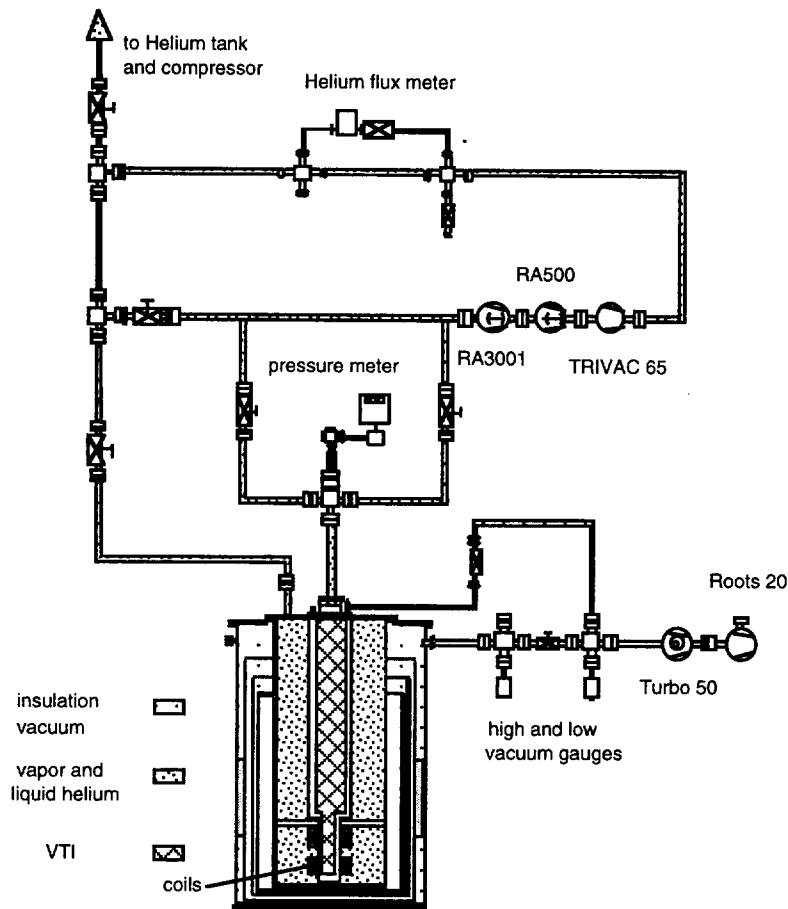


FIG. 2 – The connections of the cryostat and VTI to the helium recovery line and pumping system.

The different communications and the manually operated valves shown in Fig. 2 give the possibility to connect the VTI 1) directly to the helium gas recovery line when the target operates at $4.2 \text{ }^{\circ}\text{K}$ or 2) to the pumps whenever lower temperatures are required. The pumping system is composed by a $3000 \text{ m}^3/\text{h} + 500 \text{ m}^3/\text{h}$ RUVAC (LH RA 3001, LH RA 500) and a $65 \text{ m}^3/\text{h}$ TRIVAC (LH R 65-B).

When only the TRIVAC is switched on the He vapour pressure measured in the VTI by a pressure gauge (LH MEMBROVAC /VS) results $\approx 30 \text{ mbar}$ while the temperature of the helium bath drops down to $1.7 \text{ }^{\circ}\text{K}$. When both the RUVAC are also operating a further decrease of the temperature is obtained: $1.2 \text{ }^{\circ}\text{K}$ without MW irradiation or $2.0 \text{ }^{\circ}\text{K}$ when DNP is at work.

The power transmitted into the target region by the MW guide can be estimated measuring the flux of helium evaporating from the bath in the VTI: the full range scale of a spare fluximeter (BRONKHORST, F201C) placed at the exhaust port of the pumping system resulted, however, well below the helium flux we wanted to measure.

2.3 – The NMR signal

The calibration and measurement of the polarization is done with the Q-meter technique[8]. The polarized nucleons in the target give, in fact, a complex susceptibility $\chi(\omega)$ to the material:

$$\chi(\omega) = \chi'(\omega) - i\chi''(\omega) \quad (2)$$

where $\chi(\omega) = 0$ except for a small interval centred at the Larmor frequency ω_0 .

The polarization P of the sample is connected to the imaginary part of $\chi(\omega)$ by the relation

$$P = K \int \chi''(\omega) d\omega \quad (3)$$

where K is a constant depending from the nucleon into consideration.

If a coil is placed close to the target, the material modifies the inductance L_0 according to

$$L(\omega) = L_0 [1 + 4\pi\eta\chi(\omega)] \quad (4)$$

where η is the filling factor.

Now, since the coil is part of a series resonant RLC circuit connected to the Q meter (ULTRA-PHYSICS) by a cable of length $n\lambda_0/2$ (which, at the Larmor frequency $\omega_0 = 1/\sqrt{L_0C}$, does not contribute to the impedance of the circuit), the changes in the polarization cause changes in the Q of this resonant system. These variations can be finally measured as a change in the module of the output signal amplitude.

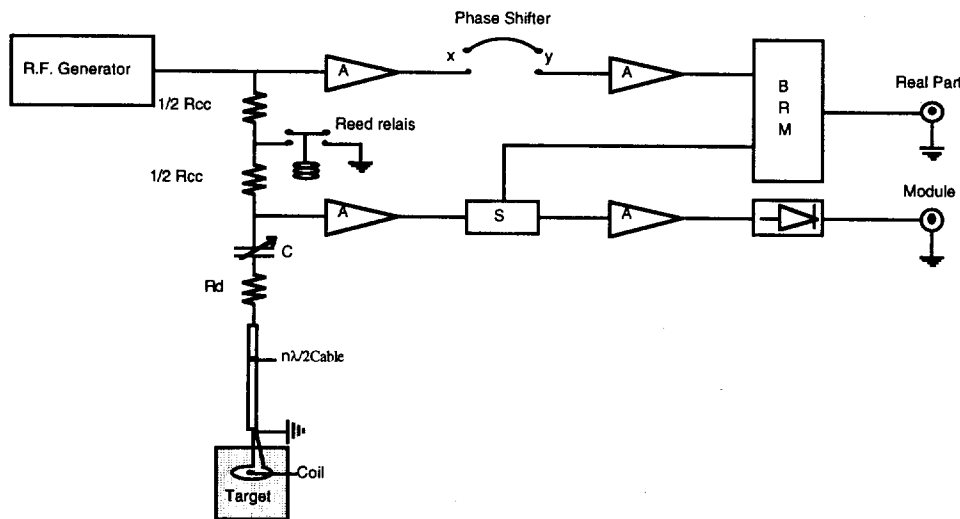


FIG. 3 – The NMR circuit to measure the polarization. The following elements are indicated: constant current resistor R_{cc} , tunable capacitor C , dumping resistor R_d , amplifiers A , splitter S and phase sensitive detector BRM . The real part and the module of the output signal are also indicated.

A simplified version of the circuit is reported in Fig. 3 . Here the RF generator (R&S SMT 02) produces a frequency sweep centred at the Larmor frequency ω_0 and 600 KHz wide. The sweep, externally triggered by a low frequency sawtooth DAC output, is sent to the Q meter which gives both the real part and the module of the signal as a function of the frequency. The real part, in particular, is directly related to the value of the polarization. Let us, in fact, define

$$S(\omega) = \text{Re}[V_{out}(\chi) - V_{out}(\chi = 0)] \quad (5)$$

where $V_{out}(\chi = 0)$ is the response obtained slightly shifting the magnetic field (baseline).

Then, at the first order,

$$\int S(\omega)d\omega \propto \int \chi''(\omega)d\omega \propto P \quad (6)$$

The measurement of the polarization is therefore performed as follow:

- the sample is placed in the helium bath at temperature T_0 and in a uniform magnetic field. The field is set to the value H_0 in order that

$$\mu H_0 = \hbar \omega_0 = h \nu_0 \quad (7)$$

where μ is the magnetic moment of the proton ($H_0 = 5$ T for $\nu_0 = 213$ MHz); the Q curve measured in these conditions is recorded.

- the magnetic field is shifted at a slightly different value $H_0 + \delta H_0$ ($\delta H_0 \cong 50$ Gauss); this baseline is also recorded.
- the integral of the difference of the two curves gives the area S_{TE} of the polarization signal at thermal equilibrium corresponding to the absolute polarization P_{TE} given in eq.(1).
- the polarization of the sample is then enhanced via the DNP using MW irradiation. The measured area S_{enh} is related to the polarization P_{enh} by:

$$P_{enh} = \frac{S_{enh}}{S_{TE}} P_{TE} \quad (8)$$

In practice, as plotted in Fig. 4b), the thermal equilibrium signal S_{TE} is very small with respect to the baseline and limited shifts on this curve due to thermal fluctuations on the NMR cable and Q-meter amplifiers cause the signal S_{TE} being still overlapped to a non-zero residual baseline as clearly shown in Fig. 4c). The effect of these thermal fluctuations has been investigated using the simulation of the response of the circuit. This approach shows that the difference of two slightly different baselines is always well approximated by a polynomial of the 3^d order. The final TE signal S_{TE} of Fig. 4d) is therefore obtained after subtraction of a 3^d order fit of the residual baseline shown in Fig. 4c) excluding a $\pm 5\sigma$ central interval, being σ the width of the TE peak.

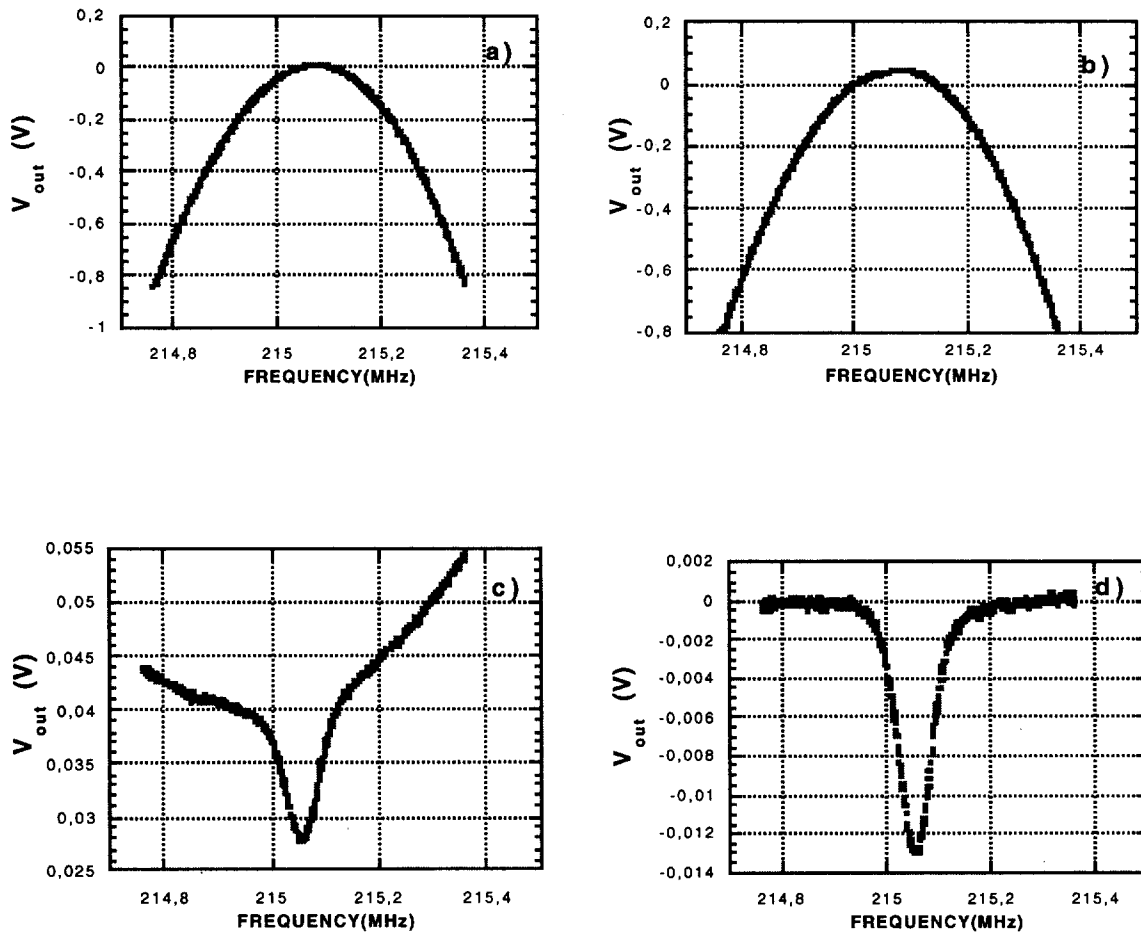


FIG. 4 – The real part V_{out} of the NMR signal in different steps of the polarization measurements. a): baseline and b): TE signal at $4.2^{\circ}K$ respectively corresponding to $V_{out}(\chi=0)$ and $V_{out}(\chi)$ in eq.5); c): difference of the two signals with evidence of the TE polarization peak; d): the TE polarization signal after the fitting procedure.

2.4 – The on-line control system

The polarized target consists of different major subsystems: the cryostat and the VTI, the superconducting magnet with its power supply, the MW generator and the NMR polarization measurement system. For the moment only the NMR and the temperature monitor on the VTI are on-line controlled.

A Macintosh QUADRA computer has been equipped with three National Ins. boards: the NB-MIO 16X analog to digital and digital to analog conversion, the NI 488.2 for GPIB

communication and the NB-DMA 2800 for direct memory access. A RS232 serial line is also connected to the Lake Shore 234 transmitter for temperature measurements.

The LabView program is used to simultaneously monitor both the polarization and the temperature of the target. A sawtooth is generated and fed via the DAC to the synthesizer connected to the NMR Q-meter and the corresponding Q-curve is digitized into 500 steps. This measurement is repeated normally 500 times (total time = $500 \times 0.05'' = 25''$) and the final average curve is plotted on the screen. Then, from the menu, the analysis on the signal can be performed (base-line subtraction and fitting) and the value of the polarization finally determined.

The automatic control of the EIO tube, pumping system, superconducting magnet supply and related monitors is in progress.

3 – RESULTS

According to eq. 8, the dynamically enhanced polarization depends from the measurement of the signal at thermal equilibrium S_{TE} . Therefore, to check the reproducibility of this signal, we kept the sample at $T=4.2 \text{ }^{\circ}K$ where the normalization procedure gives the maximum error due to the limited signal to baseline ratio. In Fig. 6 the corresponding data in one week period are reported: though the presence of some systematic error is still evident, a standard deviation of 3% among the different points (50) is obtained. During the real run, however, this result will improve: the NMR cable will in fact be screened from thermal fluctuations while the temperature of the sample is expected to be lower than $1.2 \text{ }^{\circ}K$.

The dependence of the TE peak from the temperature (eq. 1) was checked: in this measurement the temperature of the sample was lowered from 4.2 down to $1.2 \text{ }^{\circ}K$ varying the pumping speed and a correct $1/T$ behaviour was found.

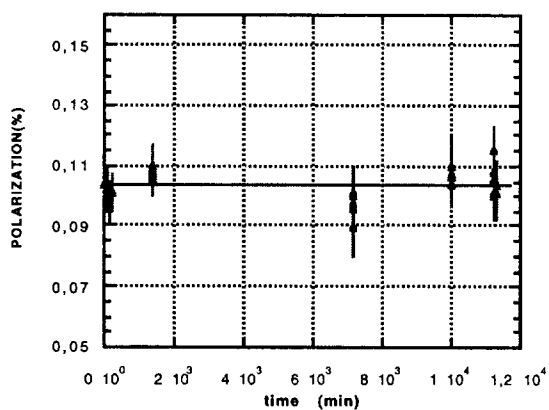


FIG. 5 – The TE polarization at $4.2 \text{ }^{\circ}K$ measured in one week period.

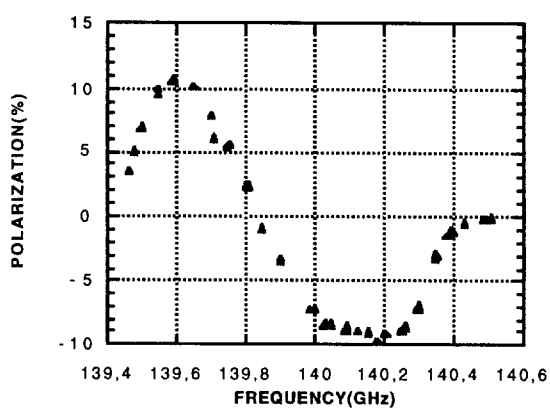


FIG. 6 – The DNP at $4.2 \text{ }^{\circ}K$ as a function of the MW frequency.

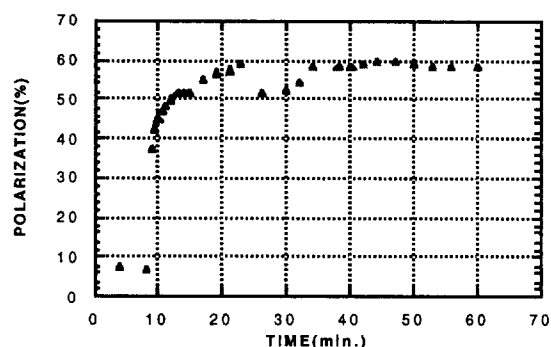


FIG. 7 – The DNP polarization at 2.0⁰ K and 139.57 Ghz; the small bump at t=25' indicates the helium filling on the VTL.

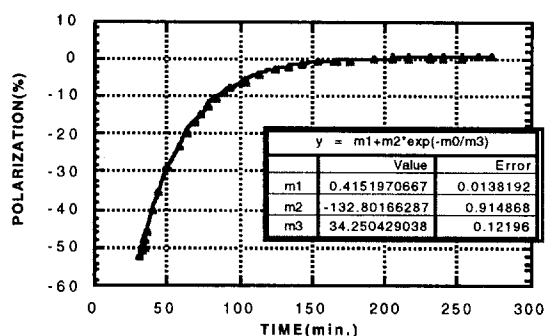


FIG. 8 – The polarization decay at 1.2⁰ K. The time is measured from the stopping of MW irradiation. The spin lattice relaxation time (SLRT) corresponds to the coefficient m3 of the fit.

To allow DNP to take place, the sample was irradiated with MW, the power released into the target region being estimated in a few hundred of mWatts. The result of a complete scanning in the MW frequency from 139.4 up to 140.5 GHz is reported in Fig 7: the maximum positive polarization (antiparallel to the magnetic field) is attained at $\nu \cong 140.2$ GHz while a maximum negative peak is observed at $\nu \cong 139.6$ GHz. During this measurement the sample was maintained in liquid helium at 4.2⁰ K; at lower temperatures the polarization increases and a maximum value $\cong 60\%$ is observed for $\nu = 139.6$ GHz and T=2.0⁰ K as seen in Fig. 7. A further increase could be in principle possible: in this case, however, a lower temperature of the sample would be required.

The spin–lattice relaxation time was also recorded at 1.2⁰ K . In this measurement the sample was polarized up to 58% using DNP; the MW was then switched off and the decay of the polarization down to its TE value was determined as reported in Fig. 8: the relaxation time of $34' \pm 1'$ results from the fit of the decay curve.

4 – CONCLUSIONS

The proton polarization of a doped butanol target was attempted using the DNP method and a maximum value $\cong 60\%$ was obtained. This result, though significantly lower than the usual reported values ($\cong 90\%$) is encouraging and compatible to the limited cooling power of our experimental set up where temperatures lower than 1.2⁰ K are not attainable.

Future progress includes polarization on irradiated ammonia and deuterated materials; the application of MW frequency modulation to increase absolute polarization is also planned.

REFERENCES

- [1] M. Taiuti et al., Nucl. Instr. and Meth. **A357** (1995) 344; P. Rossi et al., Nucl. Instr. and Meth. **A 381** (1996) 32
- [2] V.D. Burkert et al., Modern Topics in Electron Scattering, eds. B. Frois and I. Sick (World Scientific, 1991)
- [3] see, for example, PR 89–042, PR 91–023, PR 93–009, PR 93–036
- [4] B. Adeva et al., Phys. Lett. **B302** (1993) 533
- [5] Polarized Target Materials and Techniques, Nucl. Instr. and Meth. **A356** (1995)
- [6] M. Borghini, Proton Spin Orientation, CERN Yellow Report, CERN **68–32**
- [7] A. Abragam, M. Goldman, Rep. Prog. Phys. **41** (1978) 395
- [8] G. Court et al., Nucl. Instr. and Meth. **A342** (1993) 433